PHYSICAL REVIEW C

NUCLEAR PHYSICS

THIRD SERIES, VOL. 3, NO. 5 MAY 1971

Scattering of 19–30-MeV Alpha Particles from ^{16}O†

Clark Bergman* and Russell K. Hobbie

Williams Laboratory of Nuclear Physics, University of Minnesota, Minneapolis, Minnesota 55455

(Received 20 November 1970)

α-particle scattering by ^{16}O has been studied in the energy range 18.9 to 30 MeV, using the Minnesota MP tandem Van de Graaff accelerator. The target consisted of 40 $\mu g/cm^2$ of oxygen in the form of LiOH on a 20-$\mu g/cm^2$ carbon backing. Absolute cross sections were determined with an oxygen gas target. Excitation functions were measured in 20-keV steps at eight angles over the entire energy range, using computer control of the accelerator's analyzing magnet. The center-of-mass angles were selected to be zeros of the Legendre polynomials P_1 to P_8 for elastic scattering. Inelastic scattering to the 6.05–6.13-MeV doublet in ^{16}O was also studied. Elastic differential cross sections were measured at 20 energies between 18.9 and 23.0 MeV. Nonstatistical structure is observed in the excitation functions. The spins and parities of the resonances are tentatively assigned on the basis of the elastic excitation functions. A phase-shift analysis of the differential cross sections has unambiguously identified $J^\pi = 9^-$ resonances at 20.70 MeV ($\Gamma = 120$ keV) and 21.10 MeV ($\Gamma = 80$ keV) in ^{20}Ne. They may be the 9^- members of the lowest-two negative-parity rotational bands in ^{20}Ne, which are expected to be near 20 MeV.

I. INTRODUCTION

The elastic scattering of α particles by ^{16}O has previously been studied by many workers. Among these, Cameron,[1] McDermott *et al.*,[2] and Hunt, Mehta, and Davis[3] investigated the bombarding energy regions 0.94–4.0, 3.7–6.5, and 5.8–19.0 MeV, respectively.

An interesting feature of these data is the existence of resonant structure at very high excitation energies (20 MeV) in ^{20}Ne, where there are many overlapping levels. Many of these fluctuations do not appear to be statistical in origin, since they are correlated at widely spaced angles. Similar structure has been observed at high excitation energy in α-particle scattering from ^{12}C, ^{26}Mg, and other light nuclei.[4-6] Singh *et al.*[6] interpret the resonances observed in ^{30}Si via $^{26}Mg(\alpha, \alpha)^{26}Mg$ as a manifestation of intermediate structure, in which the ^{30}Si has been excited to a particularly simple configuration.

Recently, the collective motion of ^{20}Ne has received considerable attention. Extensive work at Chalk River by Litherland and others,[7] utilizing the reactions $^{12}C(^{12}C, \alpha)^{20}Ne$, $^{12}C(^{12}C, \alpha\gamma)^{20}Ne$, $^{16}O(\alpha, \gamma)^{20}Ne$, and $^{4}He(^{16}O, \gamma)^{20}Ne$, has established the existence of rotational bands in ^{20}Ne. The Florida State group has observed levels associated with several of these bands in $\alpha + ^{16}O$ elastic scattering.

The present experiment investigates $\alpha + ^{16}O$ scattering in the region from 18.9 to 30.06 MeV (19.85- to 28.7-MeV excitation in ^{20}Ne). The value of kR varies from 8 to 10 in this energy range; thus the possibility of exciting high-spin states exists. Two well-defined $l = 9$ resonances were identified by a phase-shift analysis at energies near those expected for $l = 9$ levels in known rotational bands.

II. EXPERIMENT

The Williams Laboratory MP tandem Van de Graaff accelerator provided an α-particle beam having an energy uncertainty of approximately 20 keV, and a resolution of approximately 15 keV over the energy range covered. The beam was in-

cident on a solid target, consisting of ^{6}LiOH on a 20-μg/cm^2 carbon backing. A single target containing 40 μg/cm^2 (±4%) of oxygen was used throughout the experiment. The LiOH layer degraded the incident beam by less than 16 keV. The oxygen content of this type of target remained stable for beam currents in excess of 200 nA incident on a 3-mm-diam spot. α particles scattered by oxygen are easily distinguished from those scattered by lighter target constituents for angles greater than 35°.

Eight 700-μ silicon surface-barrier detectors were used simultaneously to collect data. Rectangular slits constructed of $\frac{1}{4}$-mm tantalum defined the acceptance solid angle for each detector. The angular resolution of these detectors was ±0.25° with a typical solid angle of 0.5×10^{-3} sr. In the experiment, the angular smearing was twice this value because of the size of the beam spot. Signals produced in the solid-state detectors were amplified and transmitted to the Williams Laboratory on-line computer system for storage and further processing.[5,8] Particle identification was unnecessary because the Q values for charged-particle reactions are large and negative. The (α,p) reactions on ^{12}C and ^{16}O were potentially the most troublesome; these cross sections fortunately are quite small. At forward angles, protons with energies comparable with the α particles of interest were not stopped in the detectors.

Excitation functions were measured in 20-keV steps between 18.9 and 30.06 MeV for both ^{16}O-$(\alpha,\alpha)^{16}$O elastic scattering and for inelastic scattering to the 6.05-MeV (0^+)–6.13-MeV (3^-) doublet in ^{16}O. The detectors were placed at c.m. angles for elastic scattering which correspond to zeros of the Legendre polynomials P_1 to P_8. Runs were first made in 500-keV steps to obtain points which could be used to check consistency when the finer steps were taken. An automatic control system[9] facilitated beam-energy changes.

The average deviation of the 20-keV data from each 500-keV "check point" was −0.4%. This indicates that the oxygen component of the target was stable and that no serious malfunctions occurred.

Angular distributions were measured in 2° steps for energies every 250 or 500 keV between 18.9 and 23.0 MeV. Particular attention was paid to energies between 19.5 and 21.6 MeV, where sharp resonances had been observed in the excitation functions: Angular distributions in that range were measured every 25–50 keV.

Some of the early runs showed data scatter which was traced to twisting of the target support shaft when the lower lid of the chamber was rotated.[10] Corrections were made to early data, and careful technique eliminated the problem in later runs.

TABLE I. Normalization cross sections measured with gas cell.

θ_{lab} (deg)	$\theta_{c.m.}$ (deg)	$\sigma(\theta_{c.m.})$ (mb/sr)
140.1	149.4	47.5 (±3%)
145.0	153.3	51.35 (±3%)

Absolute cross sections were obtained by comparison with measurements at 23.12 MeV using a gas target. At this energy the cross section varies slowly with energy. The target and detector system were similar to those used by Jacobs,[11] except that the gas cell was 5 cm in diam. Runs were made with an incident beam energy of 23.58 MeV. The beam was degraded by 330 keV in the 2.5×10^{-4}-cm Havar window and by 130 keV in traversing the O_2 gas to the center of the cell. The energy resolution of the beam was about 50 keV, due to beam resolution, target thickness (≈15 keV), and straggling in the Havar and oxygen (≈30 keV). Runs were made at laboratory angles of 140.1 and 145.0°. The first angle corresponds to one used during the excitation-function measurements, and the second to a peak in the angular distribution. Table I summarizes the results of these measurements. It is felt that the 3% error covers uncertainties in charge collection and the effects of multiple scattering, as well as the 1% statistical uncertainty in the number of counts. Higher-order geometrical corrections are negligible.

III. RESULTS

Excitation functions are shown in Figs. 1–3. The data were normalized to 47.5 (±3%) mb/sr at 23.12 MeV and an angle of 149.4° (c.m.). The uncertainty in yield may be estimated by treating the error in the number of counts (approximately 5% at 10 mb/sr) and the 2% uncertainty in beam-current-integrator stability as independent statistical errors. In addition there is a normalization uncertainty of approximately 4%. This is due to 2% counting statistics at the normalization point, a 2% uncertainty in the current-integrator calibration, and the 3% uncertainty in the normalization cross section. The inelastic data have an additional uncertainty of about 10%, due to difficulties in extracting the 6.1-MeV doublet from nearby peaks.

Some of the differential cross sections are shown in Fig. 4. The cross section measured at 18.9 MeV is in general agreement with the measurements of Hunt, Mehta, and Davis[3] at the same energy. The Florida State measurements are approximately 10% lower than those made in the

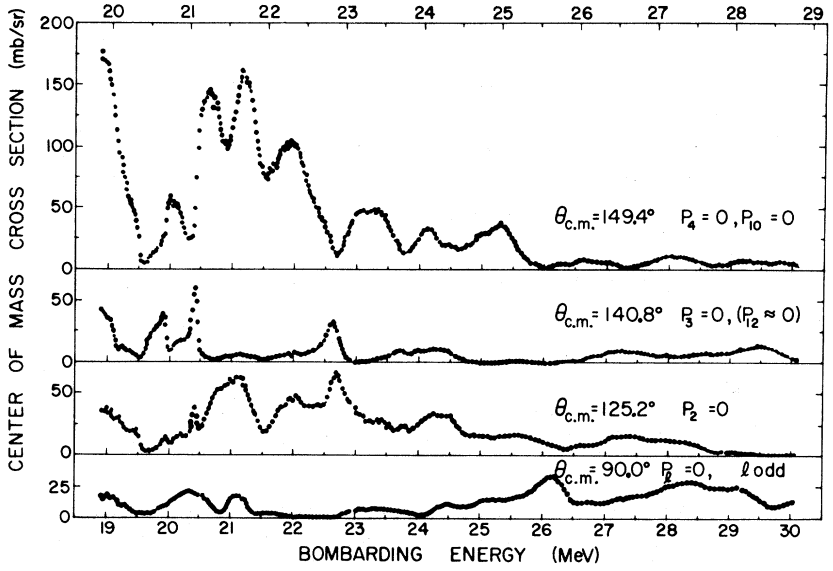

FIG. 1. Excitation functions $^{16}O(\alpha,\alpha_0)^{16}O$.

present experiment. Our data were normalized to 51.35 mb/sr at 153.3° (c.m.) and 23.14 MeV. The normalization error is 4%, while the statistical error is approximately 5% at 10 mb/sr.

IV. ANALYSIS AND DISCUSSION

The excitation functions reveal a number of prominent fluctuations having widths of 0.1 to 1 MeV (lab). The structure between 18.9 and 26 MeV is reminiscent of that observed by the Florida State group[3] from 10 to 19 MeV. One notes correlations in the fluctuations of the excitation functions at widely separated angles. Between 19 and 23 MeV there is a tendency for the inelastic cross section to the 6.1-MeV doublet in ^{16}O to be low when the elastic cross section is high and vice versa. Especially noteworthy are the two sharp dips in the inelastic cross section at 19.96 and 20.40 MeV for laboratory angles near 155°. Corresponding resonances are seen in the elastic cross section. This is the sharpest structure observed ($\Gamma \approx 80$ keV), even though the resolution

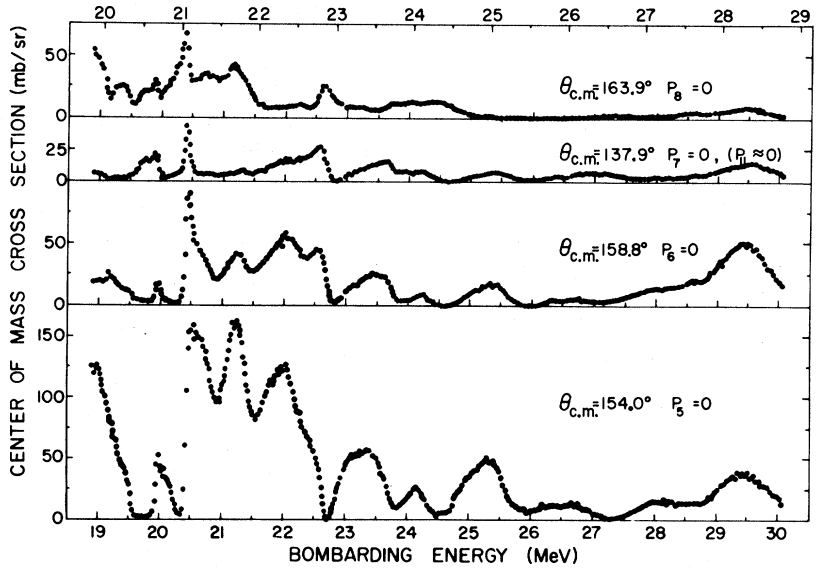

FIG. 2. Excitation functions $^{16}O(\alpha,\alpha_0)^{16}O$.

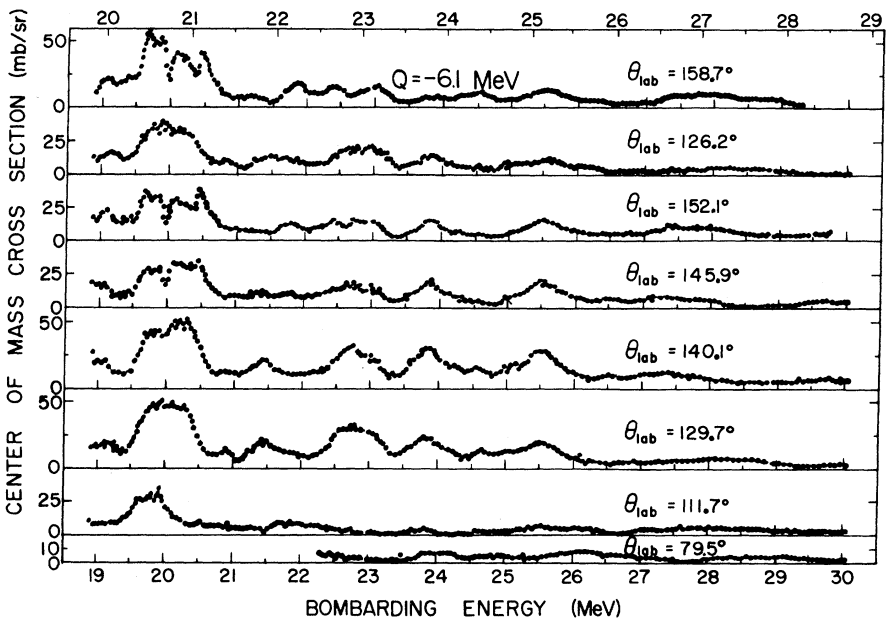

FIG. 3. Excitation functions $^{16}O(\alpha,\alpha_{12})^{16}O^*$.

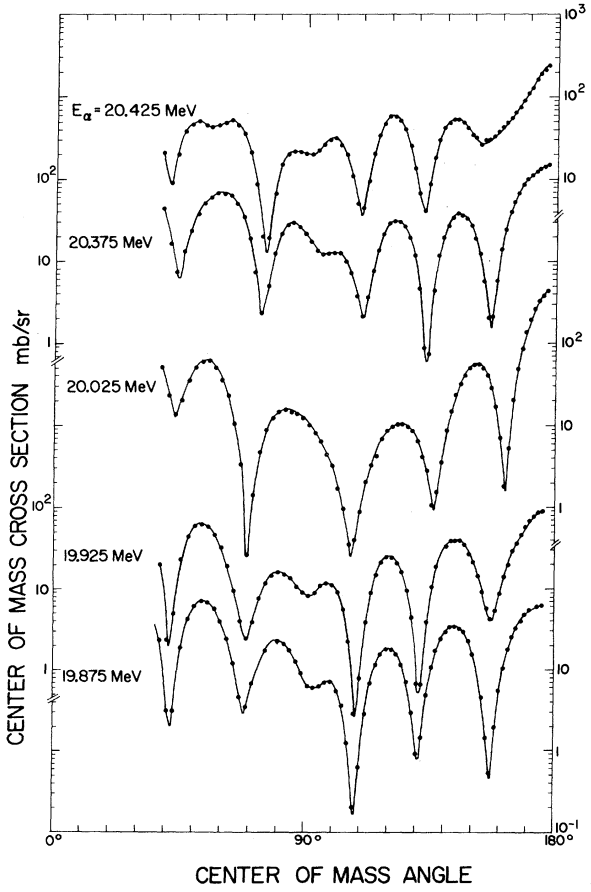

FIG. 4. Typical differential cross sections.

and step size employed would have allowed observation of structure with a width as low as 20 keV.

Above 26 MeV, fluctuations in both the elastic and inelastic cross sections diminish. Fluctuations in the elastic channel do not appear to be as well correlated for different angles as at lower energies. The inelastic cross section is small and almost devoid of structure. A broad resonance in the elastic cross section at 29 MeV is an exception to the general trend.

It appears likely that much of the observed structure is due to excitation of a relatively small number of partially overlapping compound-nuclear states. The observed cross correlations between the elastic and inelastic channels, as well as correlations between excitation functions at widely separated angles, are not expected for the statistical fluctuations described by Ericson and Brink and Stephen,[12] and Allardyce *et al.*[13] A meaningful statistical analysis of our data is not possible, since the number of statistically independent points ($\approx\Delta E/\langle\Gamma\rangle$) is too small.

A qualitative comparison of the present data with α scattering by other even-even nuclei at comparable compound-nucleus excitation energies shows the following: (1) The structure observed[5] in ^{12}C is somewhat broader and perhaps less well correlated at widely spaced angles than for ^{16}O. (2) There is a definite trend toward narrower structure ($\frac{1}{2}$ to $\frac{1}{4}$ the widths observed in this experiment) with targets of higher mass. ^{32}S and ^{40}Ca excitation functions[14,15] are examples of this be-

havior. The ^{32}S and ^{40}Ca excitation functions appear to be uncorrelated at different angles, suggesting that the structure may be due to Ericson fluctuations.

The differential cross sections show well-defined diffraction oscillations. Strong backward peaking is evident; the Coulomb cross section is sometimes exceeded by a factor of 10^3. This is characteristic of light targets and is presumably due to exchange scattering.

Phase-Shift Analysis

The elastic scattering cross section for spin-zero particles above the inelastic threshold may be written

$$\sigma(\theta) = \left| \eta \operatorname{cosec}^2 \tfrac{1}{2}\theta \exp[-2i\eta \ln(\sin \tfrac{1}{2}\theta)]/2k - i\sum_{l=0}^{\infty} \frac{2l+1}{2k} e^{2i\omega_l}[1 - A_l e^{2i\delta_l}] P_l(\cos\theta) \right|^2 ,$$

where

$k = p/\hbar$,

$\eta = Z_1 Z_2 e^2/\hbar v$,

v = the relative velocity of the particles,

$\omega_l = \sum_{m=1}^{l} \tan^{-1} \frac{\eta}{m}$;

$\omega_0 = 0$ is the Coulomb phase shift,

A_l = the absorption coefficient $(0 \leq A_l \leq 1)$,

δ_l = the real part of the nuclear phase shift.

For all practical purposes, the sum over l terminates for $l = l_{\max}$. The barrier penetration of partial waves with $l > l_{\max}$ is negligible. Thus $\delta_l = 0$ and $A_l = 1$ for $l > l_{\max}$. In this experiment, $l_{\max}$ is between 10 and 12.

One can gain some preliminary insight by a visual inspection of the excitation functions. The energies and widths of all but the very weak resonances appear in Table II. The energies may be in error by as much as $\frac{1}{2}$ the width. Visual inspection of the excitation functions yielded spin and parity assignments for the more prominent structures. The following criteria were employed to make the assignments in Table II. The lth partial wave does not contribute to the cross section at angles where $P_l(\cos\theta) = 0$. For elastic scattering of spin-zero particles, the conservation of angular momentum allows only the partial wave with $l = J$ to form a compound state with spin J. Thus, the disappearance of an anomaly at an angle where $P_l = 0$ is a necessary (but not sufficient) condition to assign a spin $l = J$. Because the intrinsic states of ^{16}O(g.s.) and the α particle have positive parity, only natural-parity states may be formed. The three 9^- assignments are the most definite.

TABLE II. Observed ^{20}Ne levels.

E_{lab} (MeV)	$E(^{20}\text{Ne}^*)$ (MeV)	J^π a	J^π b	Estimated Γ (keV)
19.30	20.15	7^-		250
19.6	20.4		6^+	360
19.6	20.4		7^-	200
19.95	20.70	9^-	9^-	120 [b]
20.18	20.85			
20.4	21.05		7^-	200
20.45	21.10	9^-	9^-	80 [a,b]
20.60	21.30			
21.20	21.70	7^-		250
21.95	22.30	7^-		400
22.5	22.7		9^-	500
22.65	22.85	9^-		250
23.2	23.3	8^+		500
24.2	24.1	8^+		300
25.4	25.0	8^+		600
26.2	25.7			400
28.1	27.2			700
29.4	28.3	10^+		700

[a] Information obtained from inspection of $^{16}\text{O}(\alpha,\alpha)^{16}\text{O}$ excitation functions.

[b] Information from the phase-shift analysis.

The numerical phase-shift analysis employed a nonlinear least-squares routine developed by Stryk.[16] Starting parameters were obtained from the smooth-cutoff model,[17] in which the phase shifts are parametrized by

$$A_l = [1 + e^{(l_A - l)/\Delta l_A}]^{-1},$$

$$\delta_l = \delta_0 [1 + e^{(l - l_\delta)/\Delta l_\delta}]^{-1}.$$

A fit for $E_\alpha = 21.50$ MeV was obtained by first setting $\delta_0 = \pi/2$, and making a grid search over the remaining four parameters to minimize χ^2. This gave $l_A \approx l_\delta \approx 7$ and $\Delta l_\delta \approx 0.1$. A further variation of these parameters did not appreciably improve the fit. The best fit had peaks at approximately the correct angles, but their relative heights disagreed badly with the experimental data.

It is well known that there exist many equivalent sets of phase shifts for a given differential cross section.[18] Because this smooth-cutoff-model starting point was very poor, one is not assured of obtaining the correct phase shifts. Nevertheless, the following program was carried out.

The first procedure was to randomly select a single partial wave with $0 < l < 8$ to reduce χ^2 by repeated simultaneous changes of A_l and δ_l. Fitting was terminated when the reduction in χ^2 became small. Many different sets of phase shifts were produced which fit the data nearly equally well.

Often one obtained $A_l > 1$ for some of the lower partial waves, for which A_l should become very small.

The next approach was to vary parameters associated with the highest partial wave $l = l_{max}$. When no further improvement could be obtained, the next lower partial wave, $l' = l - 1$, was tried. Then random choices were made among all the partial waves $l' \leq l \leq l_{max}$ until no further improvement occurred. Then l' was decreased by 1 and the procedure was repeated. A set of "reasonable" phase shifts was obtained at 21.5 MeV by starting with $l_{max} = 8$. These phase shifts provided the starting point for a search at 21.25 MeV, where the same procedure was followed. This method failed at energies near the sharp resonance at 20.40 MeV, unless the $l = 9$ partial wave was included. This method was continued at successively lower energies down to 18.9 MeV. However, when we used the lowest-energy phases as a starting point for fits at successively higher energies, the phases did not agree with those obtained on the search downward in energy.

The fitting routine was further modified to select the partial waves having the largest values of $|\partial(\chi^2)/\partial(A_l e^{2i\delta_l})|$ for fitting. Phase shifts for up to three partial waves could be varied simultaneously. Fits were made over the sharp 9^- resonance (at 20.40 MeV) by first stepping up, then down, in energy. The $l = 9$ partial wave always had the largest derivative near this resonance. In general, the phase shift obtained during fits made at successively greater energies agreed with those obtained with decreasing energy. In cases where the shapes of adjacent differential cross sections were quite different, the fitting program had more difficulty. Rather large changes in several phase shifts could occur, and the fit converged slowly. In those cases, allowing more than one partial wave to vary at a time appeared to produce more well-behaved phase shifts. That is, the A_l were more likely to remain less than 1, and hysteresis was less pronounced in the plots of phase shift vs energy. Phase shifts generated by a simultaneous variation of two partial waves, starting at 18.9 MeV and going up to 23.0 MeV, are shown in Fig. 5.

Additional differential-cross-section measurements every 25–50 keV were made in the energy range 19.50 to 20.55 MeV. The finer steps were made at energies where the excitation functions vary rapidly. These data were fit in the manner outlined above, varying two partial waves at a time. Starting at 20.55 MeV, fits were made at successively lower energies. Upon reaching 19.50 MeV, fits were made at successively higher energies. Five complete passes were made over this

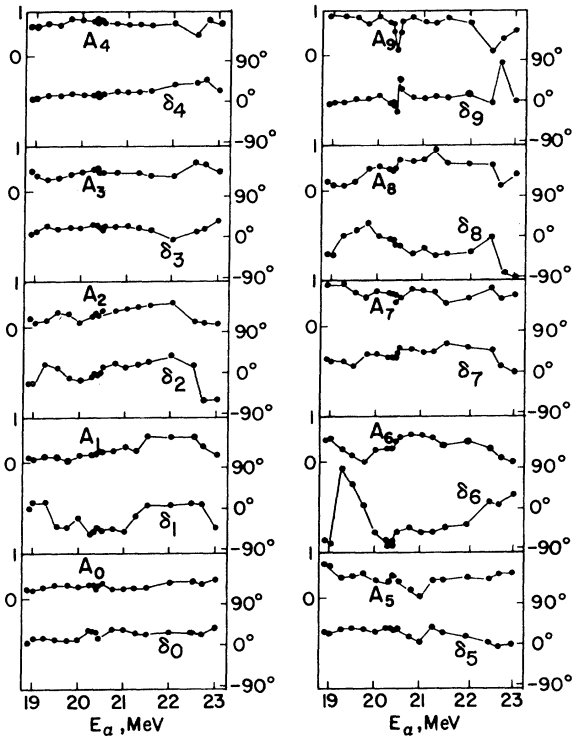

FIG. 5. $^{16}O(\alpha,\alpha)^{16}O$ phase shifts in the energy range 18.9 to 23 MeV (coarse steps).

energy range. Figure 6 shows the phase obtained on the third pass. Generally, the higher l phases were fairly reproducible. The phase below $l = 3$ or 4 was not very consistent. This might be expected because of the strong absorption of low angular momentum partial waves. For A_l small, $A_l e^{2i\delta_l}$ is quite insensitive to the value of δ_l. Also, the $2l + 1$ statistical factor makes the cross section relatively less sensitive to the lower partial waves.

The two well-defined resonances near 20.0 MeV in the excitation function are clearly identified by the phase-shift analysis as $l = 9$ (Fig. 6). Figure 5 indicates that the resonance near 22.7 MeV (22.85 MeV in ^{20}Ne) may also be $l = 9$. The importance of having data at closely spaced intervals is illustrated by the different behavior of the $l = 9$ phases near 20.0 MeV in Figs. 5 and 6. The $l = 9$ resonance at 19.95 MeV is not apparent in Fig. 5, where the cross sections were measured every 250 keV. The reproducibility of fits is also likely to be better when data are available in fine steps across resonances.

A number of other less-prominent, unresolved resonances appear between 19.5 and 20.5 MeV. Resonances occur at 19.6 MeV for both $l = 6$ and 7, and at 20.4 MeV in the $l = 7$ phases. These resonances are not as clearly defined as the $l = 9$ reso-

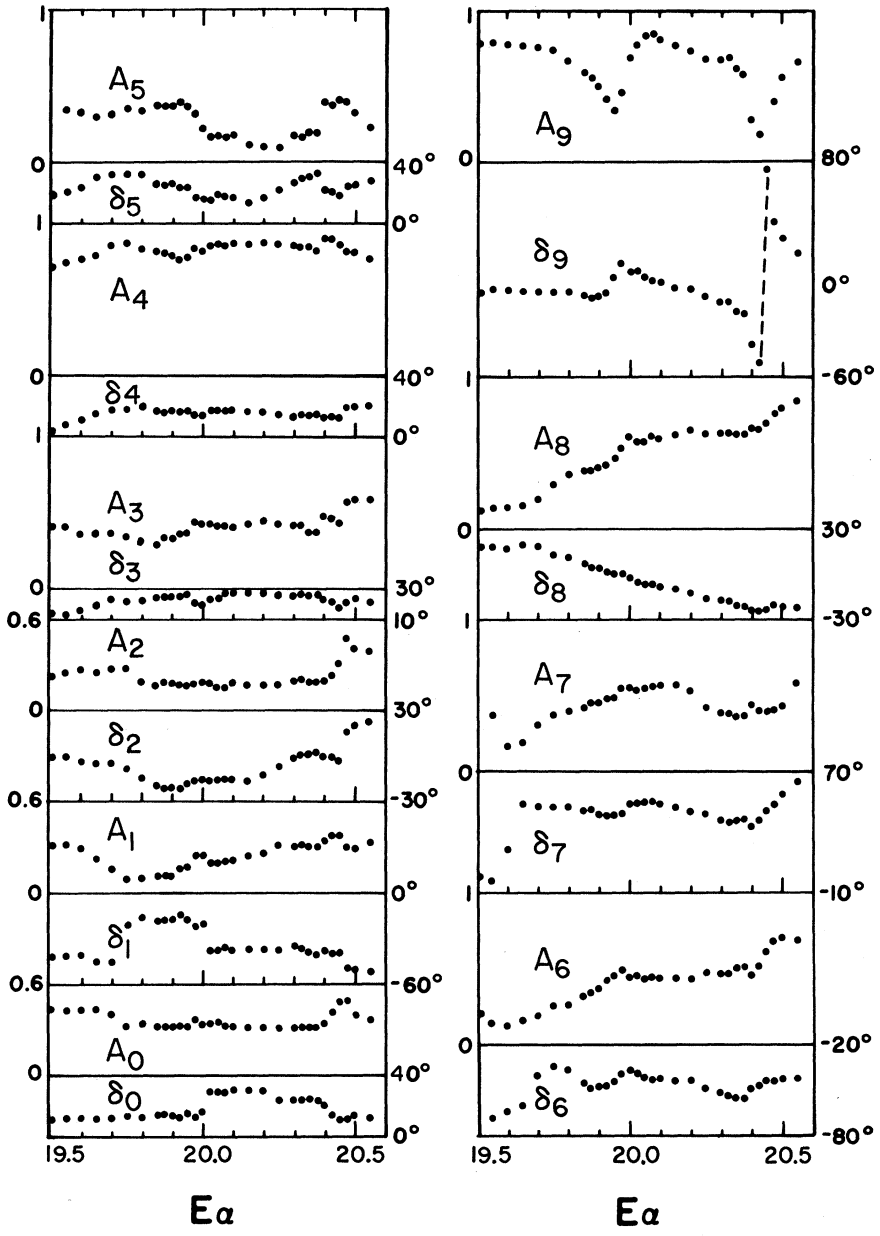

FIG. 6. $^{16}O(\alpha,\alpha)^{16}O$ phase shifts in the energy range 19.50 to 20.55 MeV (fine steps).

nances, and no conclusive identifications can be made. Many resonances occur in the energy range covered by the excitation function measurements which possibly could be identified by a phase-shift analysis of suitable data.

V. ROTATIONAL STRUCTURE OF ^{20}Ne

Low-lying levels in ^{20}Ne are known to possess a well-defined rotational structure.[7] Of particular interest here are two negative-parity rotational bands: one built on the 4.97-MeV (2^-) level and the other on the 5.80-MeV (1^-) level in ^{20}Ne.[7] These bands are shown in Fig. 7, along with the newly discovered 9^- levels at 20.70 and 21.05 MeV, respectively. If a $J(J+1)$ energy dependence for members of these bands is assumed, the 9^- levels would occur in the vicinity of 19 to 22 MeV in ^{20}Ne.

For a pure rotator, the intrinsic nuclear state is the same for all members of a given band. The partial decay width of a compound state into the channel λl is related to the reduced width γ_λ^2 by

$$\Gamma_{\lambda l} = 2kP_l\gamma_\lambda^2 .$$

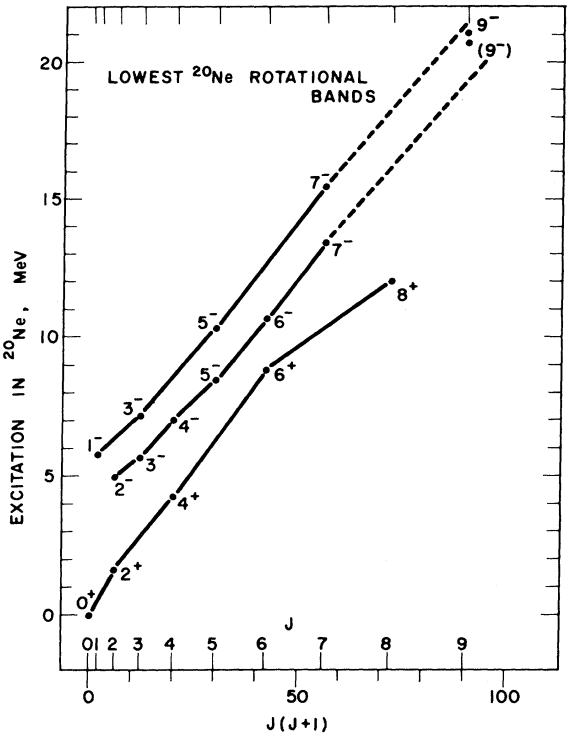

FIG. 7. Rotational bands in ^{20}Ne.

In this equation, k is the wave number and P_l is the penetration factor in the channel λ. Teichmann and Wigner[19] estimate that

$$\gamma_\lambda^2 \leq \frac{3}{2}\frac{\hbar^2}{\mu R},$$

where μ is the reduced mass and R the interaction radius in the channel λ. Kuehner and Almqvist[7] have calculated reduced widths, in units of the Wigner limit for several members of these negative-parity bands. These results, along with the reduced widths of the newly discovered 9^- levels are given in Table III. The interaction radius was taken to be 5 F. The estimated reduced widths of the 20.70- and 21.05-MeV levels are essentially the same. Both levels have reduced widths consistent with their being members of the band based on the 4.97-MeV (2^-) level. The reduced width of the tentative 9^- level at 22.85 MeV also has a reduced width comparable to that of these two 9^- levels.

TABLE III. ^{20}Ne α-particle reduced widths. E^* is the excitation in ^{20}Ne. γ_α^2 is calculated by dividing column 3 by column 4.

E^* (MeV)	J^π	$\Gamma_{\alpha l}$ (keV)	$2kP_l\frac{3\hbar^2}{2\mu R}$ (keV)	γ_α^2	Ref.
5.62	3^-	2.0×10^{-6}	42×10^{-6}	0.05	7
8.46	5^-	<0.2	6.5	<0.03	7
13.39	7^-	<40	120	<0.33	7
20.70	9^-	120	450	0.27	Present exp.
21.10	9^-	80	530	0.15	Present exp.
5.79	1^-	$>13\times10^{-3}$	24×10^{-3}	>0.54	7
7.17	3^-	8	9	0.89	7
10.30	5^-	150	142	1.06	7
15.43	7^-	376	475	0.79	3
22.85	9^-	250	991	0.25	Present exp.

VI. SUMMARY

More than 10 compound-nuclear resonances have been observed in ^{20}Ne between 19.85 and 28.7 MeV. These resonances appear to correspond to states with spin between 7 and 10. A phase-shift analysis has shown that states at 20.70, 21.10, and 22.85 MeV in ^{20}Ne have $J^\pi = 9^-$. The lower two states may be members of the two negative-parity rotational bands which have been reported previously. It should be possible to identify some of the other resonances in the same way if more closely spaced angular distributions become available.

VII. ACKNOWLEDGMENTS

We greatly appreciate the countless times the staff of the Williams Laboratory of Nuclear Physics has aided the progress of this work. Special thanks are due Dr. David C. Weisser and Dr. James F. Morgan, as well as Daniel H. Fitzgerald, Peter Mailandt, and Robert Snyder for their diligent and skillful help in collecting data.

†Work supported in part by the U. S. Atomic Energy Commission (Report No. COO-1265-87).

*Present address: Control Data Corporation, Minneapolis, Minnesota.

[1]J. R. Cameron, Phys. Rev. 90, 839 (1953).

[2]L. C. McDermott, K. W. Jones, H. Smotrich, and R. E. Beneson, Phys. Rev. 118, 175 (1960).

[3]W. E. Hunt, M. K. Mehta, and R. H. Davis, Phys. Rev. 160, 782, 791 (1967).

[4]E. B. Carter, G. E. Mitchell, and R. H. Davis, Phys. Rev. 133, B1412 (1964).

[5]J. F. Morgan and R. K. Hobbie, Phys. Rev. C 1, 155 (1970).

[6]P. P. Singh, B. A. Watson, J. J. Kroepfl, and T. P. Marvin, Phys. Rev. Letters 17, 968 (1966).

[7]A. E. Litherland, J. A. Kuehner, H. E. Gove, M. A. Clark, and E. Almqvist, Phys. Rev. Letters 7, 98 (1961); J. A. Kuehner and E. Almqvist, Can. J. Phys. 45, 1605 (1967). Many other references are given in these papers.

[8]R. K. Hobbie and R. W. Goodwin, Nucl. Instr. Methods

52, 119 (1967); R. K. Hobbie, Williams Laboratory, U. S. Atomic Energy Commission Report No. COO-1265-44 (unpublished).
[9]C. Bergman and R. K. Hobbie, Rev. Sci. Instr. 40, 1079 (1969).
[10]C. Bergman, Ph.D. thesis, University of Minnesota, 1968 (unpublished).
[11]C. Jacobs, M.S. thesis, University of Minnesota, 1968 (unpublished). C. Jacobs, J. H. Williams Laboratory of Nuclear Physics, University of Minnesota, Annual Report, 1967 (unpublished).
[12]T. Ericson, Ann. Phys. (N.Y.) 23, 390 (1963); D. M. Brink and R. O. Stephen, Phys. Letters 5, 77 (1963).
[13]B. W. Allardyce *et al.*, Nucl. Phys. 85, 193 (1966).
[14]J. P. Aldridge, C. E. Crawford, and R. H. Davis, Phys. Rev. 167, 1053 (1968).
[15]C. P. Robinson, J. P. Aldridge, J. John, and R. H. Davis, Phys. Rev. 171, 1241 (1968).
[16]R. Stryk, Ph.D. thesis, University of Minnesota, 1966 (unpublished).
[17]J. A. McIntyre, K. H. Wang, and L. C. Becker, Phys. Rev. 117, 1337 (1960).
[18]N. P. Klepikov, Zh. Eksperim. i Teor. Fiz. 41, 1187 (1961) [transl.: Soviet Phys.-JETP 14, 846 (1962)].
[19]T. Teichmann and E. P. Wigner, Phys. Rev. 87, 123 (1952).

PHYSICAL REVIEW C VOLUME 3, NUMBER 5 MAY 1971

Neutron Capture Cross Sections of ^{13}C and ^{16}O†

B. J. Allen
Australian Atomic Energy Commission, Lucas Heights, Australia, and Oak Ridge National Laboratory, Oak Ridge, Tennessee 37830

and

R. L. Macklin
Physics Division, Oak Ridge National Laboratory, Oak Ridge, Tennessee 37830
(Received 2 December 1970)

Measurements have been made of the radiative widths of the lowest energy resonances in ^{13}C and ^{16}O. Maxwellian-averaged capture cross sections calculated for $kT = 30$ keV indicate that ^{13}C and ^{16}O could not have been significant neutron poisons in s-process nucleosynthesis.

The neutron capture cross sections of ^{13}C and ^{16}O are of astrophysical interest in the keV energy range. Because of their high abundances, these isotopes could act as significant neutron poisons if their capture cross sections were sufficiently high. Nucleosynthesis by slow-neutron capture (i.e., the s process[1]) starts near ^{56}Fe, which would therefore compete with these lighter isotopes for the available neutrons. If this were indeed the case, it might also be possible to set an upper limit to the neutron temperature compatible with the observed s-process buildup.

Measurements of the capture cross sections of ^{13}C and ^{16}O have been made at the Oak Ridge linear accelerator.[2] The accelerator was pulsed at 800 pulses/sec, with a beam-pulse width of 50 nsec. Operating power was 24 kW. Targets used were a 1-g 58% enriched sample of ^{13}C and a 99.992% enriched $^{7}Li_2CO_3$ sample which yielded data on both ^{16}O and ^{7}Li. Measurements were made at 40 m,[3] with a pair of total-energy detectors (TED) which have been described previously.[4] Two 4.1-in. fluorocarbon liquid scintillator cells (NE 226) flanked the sample when it was in the 2×1-in. collimated neutron beam. The pulse-height weighting technique[4] was not used in these measurements and consequently the detector efficiency was sensitive to the shape of the resonance-capture spectrum. However, the detector response function is relatively independent of the spectrum shape, and an over-all systematic error of 30% is estimated to include this effect.

Capture yields were normalized relative to the iodine capture cross section. A PbI_2 sample was used for this purpose; corrections were made for the time-dependent background as determined by a graphite scatterer and the black-resonance-transmission technique. In the latter case the yield after transmission through a 5-cm pressed sulphur filter at the 105-keV resonance gave an estimate of the time-dependent background as observed with the PbI_2 sample. The time-of-flight spectrum was also calibrated in this measurement using the energies of sulphur resonances as listed by Garg *et al.*[5]

The discriminator levels for the TED's were set at ~0.12 MeV for the ^{13}C/PbI_2 comparison. Thus, inelastic scattering to the 57.6-keV level in iodine did not contribute to the iodine yield, and the 153-keV ^{13}C resonance lay below the second inelastic